Calculation of Muzzle Blast Flowfields

J. I. Erdos* and P. D. Del Guidice†
Advanced Technology Laboratories, Westbury, N.Y.

The muzzle blast field generated by a gun-launched high-velocity projectile is characterized by a highly underexpanded supersonic exhaust plume, which terminates at a strong shock (the Mach disk), an expanding front of exhaust gases (the contact surface), and an expanding, nearly spherical outer shock (the blast wave). The present study is directed toward theoretical description of the inviscid gas dynamics of the blast field. The noted features are discussed in terms of well-established theories for spherical blast waves with variable energy release and for steady underexpanded plumes, from which their interaction can be qualitatively described. To obtain a quantitative representation, a finite difference solution is developed for the unsteady compressible flow between the Mach disk and the blast wave, assuming spherical symmetry. The results obtained are in good agreement with experimental measurements of the motion of the blast wave, the contact surface and Mach disk for a 3200 fps round fired from an M16 rifle.

Nomenclature

a = speed of sound, $(\gamma p/\rho)^{1/2}$
B = a constant related to energy content of blast field
C_p = specific heat at constant pressure
d = bore diameter
E = energy
i = an index: $i=1$ for propellant gas, $i=2$ for air
j = an index: $j=0$ for planar symmetry, $j=1$ for axial symmetry, and $j=2$ for spherical symmetry
k = arbitrary constant
M = Mach number
n = exponent of time in blast wave theory for shock position
p = pressure
r = radial distance
S = entropy
t = time
u = gas velocity
z = axial distance
z_o = origin of a spherical coordinate system
β = exponent of time for description of energy variation in blast wave theory
γ = ratio of specific heats, C_p/C_v
θ = polar angle
ρ = gas density
λ = independent variable in blast wave theory

Subscripts

c = contact surface
e = nozzle exit
p = projectile
r = reference condition
s = shock (Mach disk or blast wave)
∞ = ambient (freestream) value

Introduction

THE present study is motivated by interest in the aerodynamics of sabot discard within the environment of the muzzle blast field (usually termed the transitional or intermediate ballistics regime) for a gun-launched supersonic projectile.[1] The acoustic and optical (i.e., flash) characteristics of muzzle blast are also of practical concern. Definition and modeling of the unsteady gas-dynamic processes that occur within the blast field are necessary prerequisites to analysis of these and other related problems, and constitute the subject of the present paper.

Descriptions of the gas dynamic processes that generate the muzzle blast field are available elsewhere[2,3] and the details will be only briefly reviewed here in relation to the analytical models to be described. Two blast fields are generated by each round fired; the first, or precursor, is due to the expulsion of a column of air driven out of the barrel ahead of the round, and the second is due to the release of propellant gases from the barrel after the round exits the muzzle. The visible features of these flowfields are exhibited in the shadowgraphs shown in Figs. 1 and 2, from Refs. 3 and 4. The spherical blast wave

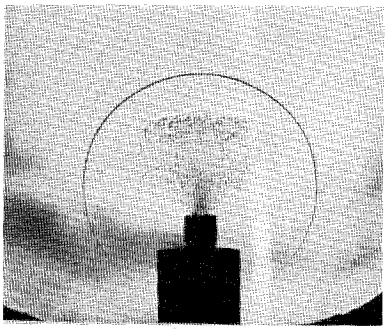

Fig. 1 Precursor blast field generated by explusion of air from the barrel by the projectile—M16 round fired from Mann barrel at 3200 fps muzzle velocity.

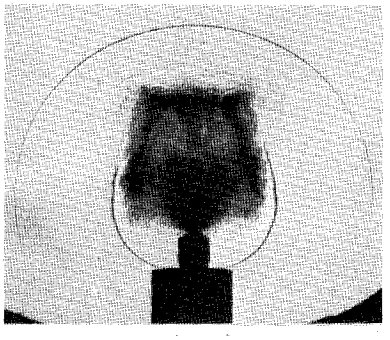

Fig. 2 Blast flowfield generated by release of propellant gases from the barrel—M16 round fired from Mann barrel at 3200 fps muzzle velocity.

Presented as Paper 74-532 at the AIAA 7th Fluid and Plasma Dynamics Conference, Palo Alto, California, June 17-19, 1974; submitted July 1, 1974; revision received April 22, 1974. Research was performed for U.S. Army Ballistic Research Laboratories under Contract DAAD05-73-C-0038. The authors are pleased to acknowledge the cooperation of E. Schmidt of BRL during this study.

Index categories: Nonsteady Aerodynamics; Shock Waves and Detonations.

*Senior Research Scientist and Vice President. Member AIAA.
†Research Scientist.

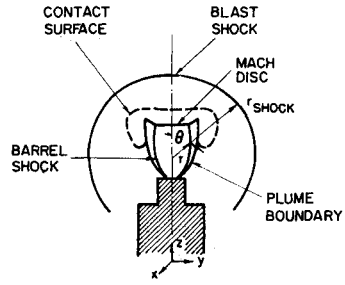

Fig. 3 Structure of precursor blast field.

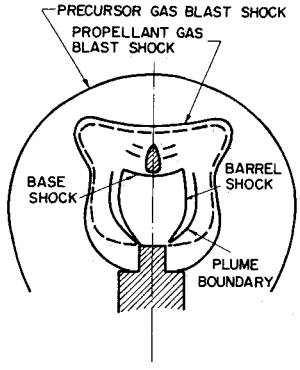

Fig. 4 Structure of propellant gas blast field.

produced in the precursor blast field is also present in the propellant blast field shown in Fig. 2. However, like all features of the precursor field, it will be overtaken, and effectively annihilated, by the blast wave produced by release of the propellant gases. The relative strength of the two fields can be indicated by noting that the precursor gas is compressed to about 16 atm by an M16 round having a muzzle velocity of 3200 fps, but the propellant gases at the muzzle are compressed to about 600 atm at the time the round leaves the muzzle. Consequently, the interaction between the precursor and propellant gas flowfields during evolution of the latter can be neglected for all practical purposes, insofar as the present study is concerned. However, the two blast fields are very analogous in terms of their structure and, therefore, the precursor flowfield can provide relevant information. In particular, the precursor field is free of perturbing effects due to the presence of the projectile in the flowfield, oxidation of the propellant gases, and obstruction of the visible features of the flow due to the presence of the projectile in the flowfield, oxidation of the propellant gases, and obstruction of the visible features of the flow due to the high density of the propellant gases.

The principal structural features of the blast field associated with the precursor gas are identified in Fig. 3. The flow contained between the plume boundaries up to the Mach disk possesses the characteristics of a highly underexpanded supersonic exhaust jet, and, for reasons to be discussed later, can be described in the framework of a steady flow. The contact surface represents the front of the gas emerging from the barrel. Considerable turbulent mixing along this surface and the plume boundary is evident in the shadowgraphs, which has a direct bearing on description of the muzzle flash, but has very limited influence on the presently considered inviscid structure of the flowfield. The blast shock is driven by the expanding front consisting of the contact surface and the plume boundary, which initially have a highly distorted (i.e., nonspherical) shape. However, as the blast shock moves away from the front the correspondence between the shock shape and the frontal shape diminishes, and the blast shock asymptotes to a spherical sound wave. It will be shown that the flowfield near the axis of symmetry between the Mach disk and the blast shock, which is herein termed the shock layer, can be approximated remarkably well as a spherically symmetric unsteady flow.

Figure 4 displays the structural features of the blast field associated with the propellant gases, at a time when the projectile is within the plume and interacting with it, and the blast shock is nearly coincident with the contact surface. At later times when the projectile has cleared the blast field, the flow structure assumes the same configuration as that shown in Fig. 3. Although the propellant gas blast field initially appears more highly distorted than the precursor blast field, the principal features of the precursor blast field are reproduced, with the possible exception of the Mach disk. A nearly normal shock is formed at the base of the projectile, which terminates the supersonic plume and precludes formation of the Mach disk. It appears from the data that the base shock falls back from the base to form the Mach disk when the pressure downstream of the normal shock corresponds to the back pressure that would exist downstream of the Mach disk in the absence of the projectile.

Blast Wave Theory

Classical blast wave theory,[5] with particular reference to variable energy blast waves,[6,7] is highly descriptive of the blast wave motion associated with expulsion of the precursor gas and with release of the propellant gas from the muzzle of a gun. The following discussion is intended to briefly review the relevant concepts and results of blast theory. It is emphasized however, that these results will be used to illustrate the salient functional relationships and their application to development of scaling laws pertinent to transitional ballistics, but are not employed in the numerical shock layer solution to be described in a following section, which also includes the blast wave motion.

Blast wave theory generally refers to the description of the motion of a gas through which a shock wave has passed, due to the release of energy at a source, under conditions for which the governing equations and boundary conditions admit a family of similar solutions. The required conditions consist of a symmetric (i.e., one dimensional) flow, negligible ambient pressure (i.e., a strong shock wave) and a power-law variation of the energy release in the flow. The most familiar example is an explosion, for which all energy is assumed to be released instantaneously (i.e., the power-law exponent is zero). The assumption of negligible ambient pressure is eventually violated as the shock decays to a sound wave, but other solutions can be found which include finite ambient pressure or are descriptive of the weak wave limit.[5] The conditions of symmetry and power-law variation of energy are the most restrictive in the present context.

The governing system of equations is reduced to a set of ordinary differential equations in terms of an independent variable λ defined by $\lambda = B r t^{-n}$, where B and n are constants. In particular, λ is defined to be unity at the shock, $r_s = B^{-1} t^n$; an inner boundary defined by $\lambda =$ constant also exists, which corresponds to the contact surface. The properties of the latter boundary are determined by an appropriate constraint on the integral properties of the flow, e.g., the total mass, momentum and energy. Present interest is placed on determination of solutions with prescribed energy content, for which there is obtained[7]

$$E = Wt^{\beta} \tag{1}$$

where

$$W = \text{constant} = B^{-(j+3)} p_{\infty} n^2 J_o / A_{\infty}^2 \tag{2}$$

$$\beta = (j+3)\, n - 2 \tag{3}$$

and $J_o(n,j,\gamma)$ is a nondimensional form of the total energy integral. The classical point source explosion solution is recovered with $j=2$ and $\beta=0$, for which $n=2/5$; however solutions for a constant rate of energy addition, $\beta=1$,

decaying rates of energy addition, $0<\beta<1$, and increasing rates of energy addition, $\beta>1$, are also admitted.

With respect to the deposition of energy by release of the propellant gas from the muzzle of a gun barrel, the energy content of the flow will be proportional to the product of the muzzle exit pressure, the bore area, the exit velocity of the propellant gas and time. Therefore

$$W=kp_e\,u_e\,\mathrm{d}^2\,t^{1-\beta}=\text{constant} \tag{4}$$

or

$$p_e\,u_e\,t^{1-\beta}=\text{constant}=p_{e_r}\,u_{e_r}\,t_r^{1-\beta} \tag{5}$$

where $(\ )_r$ refers to some suitable reference point in the energy decay curve.

The general applicability of blast wave theory to description of muzzle blast phenomenology is limited by the requirement that the variation of the product of pressure and gas velocity at the muzzle can be approximated by a single power-law during the time period of interest. Accordingly, applicability of blast wave theory to possible scaling laws for blast fields (e.g., Ref. 1) is premised on the assumption that the same power-law pertains to the considered conditions.

Experimental measurements of the blast shock trajectory along the axis of symmetry for the muzzle blast generated by an M16[3,4] are presented in Fig. 5. It can be seen that the propellant blast wave data are accurately correlated by $r_s\sim t^n$ with $n=3/5$ up to a time of about 10^2 μsec, implying a constant rate of energy addition, i.e., $\beta\simeq 1$, on this time scale. Schmidt and Shear[3] calculated the rate of energy deposition at the muzzle face based on results of an internal ballistics solution carried out at BRL. They obtained $\beta=.956$ for $t\leq 10^2$ μsec, in very close agreement with the rate indicated by the blast wave motion.

At 10^2 μsec, the shock velocity has decayed to a Mach number of approximately 1.8 for which the shock pressure ratio is about 3½. Therefore, the deviation of the data from an $n=3/5$ power-law at later times is more probably attributable to violation of the strong shock assumption of blast theory than to variation in the rate of energy deposition in the flowfield. The form of the solution for a spherically expanding weak wave is given by[5]:

$$(\mathrm{d}r/\mathrm{d}t)=a_\infty\,(1-k\,(lnr)^{1/2}/r)^{-1/2} \tag{6}$$

The unknown constant in this expression can be determined by matching this solution to the blast solution at some point in a region of mutual validity, chosen at $t=10^2$ μsec in this case. As can be seen in Fig. 5 the resulting composite spherical blast wave solution provides an excellent correlation of the data over the entire range of measurements. It is implied from this result that the flow near the blast wave is spherically symmetric and lends credence to a corresponding approximation of the entire flowfield between the Mach disk and the blast wave.

Supersonic Jet Plume Model

The gas dynamic characteristics of steady underexpanded supersonic jet plumes have been studied extensively in connection with free jets and rocket motors as well as with respect to muzzle gas flows.[1,3,4] The following discussion is intended to review briefly the salient properties of highly underexpanded plumes as they relate to modeling of the nonsteady muzzle blast flowfield.

It should be pointed out initially that the gas flow exhausting from the muzzle has a velocity that is either sonic or supersonic under the conditions of interest herein. A source-like flow pattern is produced at the muzzle, viz., the streamlines near the axis tend to continue in the axial direction while those near the outer boundary of the flow tend to diverge radially from the muzzle face. However, a radially expanding axisymmetric supersonic flow produces a continuously decreasing pressure, while the plume boundary is, at least approximately, a constant pressure surface. Therefore, the streamlines at the boundary must turn inward relative to those approaching the boundaries, resulting in formation of the barrel shock at the muzzle exit plane, (cf Fig. 3). All inward traveling (reflected) waves from the plume boundaries coalesce with the barrel shock, thereby preventing transmission of signals from the boundaries to the flow between the axis and the barrel shocks. A Mach disk as shown in Fig. 3 occurs where the pressure downstream of the shock matches the prevailing pressure field. Consequently, the outer boundaries of the plume, the barrel shocks and the Mach disk will be positioned by the exterior pressure field acting on the plume, but, significantly, the supersonic flow between the axis and the barrel shock up to the Mach disk, will be independent of the exterior pressure field. Thus, the supersonic flow on the axis of the plume will only depend on the muzzle exit conditions.

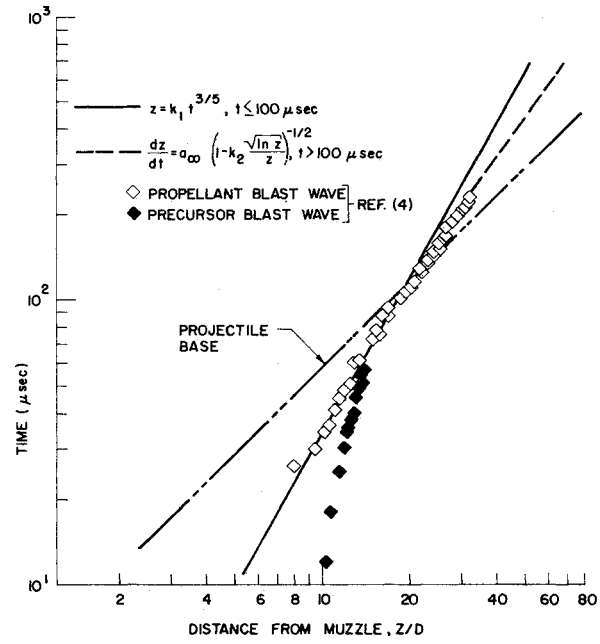

Fig. 5 Comparison of spherical blast wave theory and M16 blast wave data.

From the previously noted characteristics, it can be immediately recognized that the effects of time-varying muzzle exit conditions can change the plume axis conditions as well as affect the positions of the boundaries and the shocks. However, a time-varying exterior pressure field can change the positions of the boundaries and the shocks, but cannot alter the plume axis conditions, up to the Mach disk. Furthermore the characteristic gas transit time in the plume is typically very short compared to the time scale for the muzzle exit conditions; i.e., the supersonic plume adjusts very rapidly to variations in the muzzle exit conditions. (The same conclusion is drawn in Ref. 2). Therefore, in the present study the supersonic plume is considered quasi-steady in the sense that the flow up to the Mach disk can be accurately described at any instant by a steady flow solution based on the instantaneous muzzle exit conditions.

Several approximate, source-like solutions have been developed to describe the flow in highly underexpanded steady plumes.[2,8,9] However, the approximate solutions are generally in error near the muzzle exit, although the approximate solution of Ref. 8 approaches an exact (method-of-characteristics) solution[10] at some distance from the exit. Since the Mach number distribution in a highly underexpanded plume (between the axis and barrel shocks) only depends on the Mach number at the exit M_e and the value of γ

for the gas (assuming it is chemically frozen and not rarefied), it will be invariant as long as M_e and γ are invariant. In the experiments of Ref. 4, $M_e \simeq 1.0$ and $\gamma \simeq 1.25$ for the entire time span of interest for the propellant gas plume.‡ Thus, it is important to recognize that the Mach number distribution will not vary with time. Specifically, the time history of the pressure and gas velocity at the muzzle exit and the steady Mach number distribution[10] are sufficient to define the distribution of all flow properties along the axis of the supersonic plume at any instant.

Unsteady Shock-Layer Analysis

Although the foregoing results from blast theory provide useful information regarding the blast wave motion per se, and associated scaling laws, they do not yield a complete description of the shock layer contained between the Mach disk and blast wave. The shock layer can be considered as consisting of two sublayers; the outer layer is contained between the blast wave and the contact surface and the inner layer between the contact surface and the Mach disk. Blast theory only pertains to the outer layer. Therefore, a numerical method of analysis of the entire shock layer has been developed, and implemented in a computer program. Based on the success of spherical blast theory with respect to the blast wave motion, the entire shock layer is assumed to possess spherical symmetry. However, it should be noted that the initial flow expansion from the muzzle face into the supersonic plume can also be approximated by a spherically symmetric flow emanating from a source within the gun tube; but the barrel shocks intercept the source-like flow streamlines and turn them in the axial direction, producing a flow pattern between the barrel shocks and plume boundaries that is more nearly axial than radial, and that can only possess axial symmetry. In point of fact, most of the mass of the exhausting muzzle gas is contained in this region between the barrel shocks and plume boundaries, and relatively little is contained between the barrel shock and axis.§ Therefore, if the shock layer is to possess the spherical symmetry which it evidently attains asymptotically, it must be the result of divergence of the outer streamlines downstream of the Mach disk. Consequently, if the shock layer is modeled by a spherically symmetric source-like flow, the effective source must be located on the axis at a point upstream of the Mach disk but not necessarily within the gun tube. Thus, the supersonic plume can be envisioned as an extension of the gun in the sense that it moves the effective source of the flow in the shock layer to a point outside the actual gun tube. Estimates of the effective origin of the spherical source flow range from 2/10 of the bore diameter suggested by Oswatitsch,[2] based on divergence of the streamlines in the supersonic plume, to a value about 3/4 of the distance from muzzle face to the instantaneous Mach disk location which represents the center of circular approximations to the instantaneous blast wave contours (see Figs. 5 and 10 of Ref. 4). Examination of the shape of the blast wave contour near the axis of symmetry clearly indicates that spherical symmetry is only a rough approximation to the true shape at early times. The use of a moving source must be recognized as a heuristic method to approximate the actual three-dimensional flow by a spherically symmetric field.

The governing system of equations are therefore assumed to possess spherical symmetry in a coordinate system having a translating origin, $z_o(t)$. The statement of conservation of mass evaluated on the axis ($\theta = 0$) in a stationary frame of reference then becomes

$$\frac{D\rho}{Dt} = -\rho \left[\frac{\partial u}{\partial r} + 2 \frac{u - dz_o/dt}{r - z_o} \right] \tag{7}$$

where the operator $D/Dt = \partial/\partial t + u\ \partial/\partial r$ pertains to the stationary system, the radial distance r is measured from a fixed origin, e.g., the muzzle face, and the velocity u is correspondingly defined with respect to the stationary (gun-fixed) reference frame. The statement of conservation of momentum is invariant under the considered transformation

$$Du/Dt = -(\partial p/\partial r)/\rho \tag{8}$$

The difference in thermodynamic properties of the gases on either side of the contact surface (in the case of the propellant driven blast field) must be recognized; the statements of conservation of energy and of state are therefore given by

$$DS/Dt = 0 \tag{9}$$

where

$$p = k\rho^{\gamma_i} \exp(\gamma_i S/C_{p_i}) \tag{10}$$

$$i = 1 \text{ (for propellant gas)}, 2 \text{ (for air)} \tag{11}$$

The values of γ_i and C_{pi} are taken as constants. For the cases reported herein $\gamma_1 = 1.25$, $\gamma_2 = 1.40$, $C_{p1} = 9507$ ft^2/sec^2/°R and $C_{p2} = 6006$ ft^2/sec^2/°R. The gases are thus each assumed to behave in accord with perfect gas theory, and mixing of the gases along the contact surface, oxidation and/or combustion of the propellant gases and associated heat release, radiation, and other related phenomena are neglected. Accordingly, subscripts are not shown on the pressure, density, entropy, etc., since both Eqs. (9) and (10) are understood to apply separately to each gas. In addition, interactions beteween the projectile and the shock layer are not considered.

The set of governing partial differential equations as stated, Eqs. (7-9) cannot, of course, be applied across the surfaces of discontinuity which bound the two sublayers of the shock layer, viz., the Mach disk, the contact surface and the blast wave. The Rankine-Hugoniot equations are used to describe the jump conditions across the Mach disk and blast wave, in shock-fixed coordinates.[1] The conditions in the supersonic plume at the instantaneous location of the Mach disk provide the upstream conditions for the Mach disk, while ambient atmospheric conditions are assumed to prevail upstream of the blast wave, i.e., the interaction of the precursor blast and the propellant blast is neglected. The shock velocity is determined (iteratively) at each instant by the requirement that the downstream conditions match a compatibility condition associated with the wave reaching the shock at the same instant from within the shock layer, which will be discussed later.

The motion of the contact surface is determined by the requirement that the pressure is continuous across the contact, the velocity on the axis ($\theta = 0$) is also continuous (i.e., the tangential component is zero), and the entropy on each side is a constant. For the propellant-generated blast field, the entropy on the airside of the contact can be approximated by the entropy behind a normal shock (with $\gamma = \gamma_2$) having a pressure ratio equal to the ratio of muzzle exit pressure to ambient pressure at $t = 0$, and the entropy on the propellant side of the contact can be equated to the entropy of propellant gas at $t = 0$. (A corresponding estimate can be made for the precursor shock as it emerges from the muzzle.)

Determination of the pressure and velocity of the contact surface, and the velocity of each of the shock surfaces, is facilitated by restating the governing equations in the form of characteristic relations. Combination of Eqs. (7-9) yields

$$\frac{d\ ln\ p}{dt} \pm \frac{\gamma_i}{a} \frac{du}{dt} = -\frac{2\gamma_i}{r - z_o} \left[u - \frac{dz_o}{dt} \right] \tag{12}$$

on

$$dr/dt = u \pm a \tag{13}$$

‡ $M_e \simeq 1.51$ and $\gamma = 1.40$ prevail for the precursor plume.

§ This result can be seen from consideration of the density ratio for the two regions as well as the area ratio.

and

$$S = \text{constant} \tag{14}$$

on

$$dr/dt = u \tag{15}$$

In the present solution, second-order accuracy is achieved by locating the characteristic origin using the average of a wave speed at the point $(r,\ t+\Delta t)$ based on the first-order solution and at the origin of the characteristic $[(r-(u\pm a)\Delta t),\ t]$ based on the known solution, and correspondingly re-evaluating the average value of the right-hand side and sound speed in Eq. (12).

Note that the contact surface (or any other stream path) always represents the point of intersection of upstream and downstream running waves. Therefore, integration of Eq. (12) on the downstream running wave intersecting the contact from the propellant side ($i=1$ and $dr/dt=u+a$) and integration again on the upstream running wave intersecting the contact from the air side ($i=2$ and $dr/dt=u-a$) provides two equations which can be solved algebrically for the contact pressure and velocity, to first-order accuracy. Second-order accuracy is achieved by relocating the characteristic origin as indicated above and iterating the value of the velocity until the pressure is obtained to within acceptable accuracy. (A maximum error of 0.1% is considered acceptable in the calculations to be presented herein). The density on each side of the contact is determined from the appropriate equation of state and the known entropy.

At the Mach disk, Eq. (12) evaluated on the upstream running wave ($i=1$ and $dr/dt=u-a$) together with the shock jump equations and the known conditions on the supersonic plume axis and at the muzzle exit, provide a unique solution for the shock velocity of the Mach disk and thereby the disk location at time $t+\Delta t$. The solution is again accomplished by iteration of the shock velocity until the pressure on the downstream face of the shock is obtained to within acceptable accuracy (i.e., 0.1% error). Note that the upstream conditions in this iteration procedure also depend on the Mach disk location and, therefore, the shock velocity; however, no convergence problems have been encountered in the cases considered herein. A corresponding procedure is employed at the blast wave, using Eq. (12) on the downstream traveling wave ($i=2$ and $dr/dt=u+a$), but in this case the conditions upstream of the shock are invariant.

A combination of finite difference and characteristic techniques are employed to determine the solution of Eqs. (7-9) in the interior of the shock layer. A new coordinate system is defined that normalizes the distance between the boundaries of each sublayer

$$\xi_i = (r-z_i)/(z_{i+1}-z_i) \tag{16}$$

where $i=1$ refers to the sublayer contained between the Mach disk and contact surface (i.e., the propellant gas layer) and $i=2$ to the sublayer between the contact and the blast wave (i.e., the air layer). Accordingly z_1, z_2, and z_3 are the coordinates of the Mach disk, contact surface, and blast wave, respectively. The equations of conservation of mass and momentum, Eqs. (7) and (8), are restated in the above coordinate system and solved by the second-order finite difference scheme developed by MacCormack.[11] This algorithm is particularly convenient to implement in a computer code, and is stable when the Courant-Friedrichs-Lewy criterion is observed

$$\Delta t \leq \Delta r/(u\pm a) \tag{17}$$

which is also a necessary condition for the finite difference solution to converge to a solution of the differential equations as $\Delta r \to 0$.

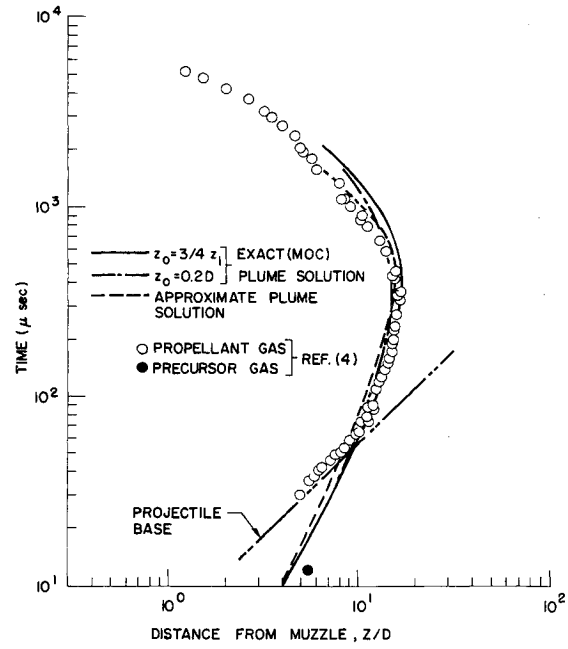

Fig. 6 Mach disk trajectory for M16.

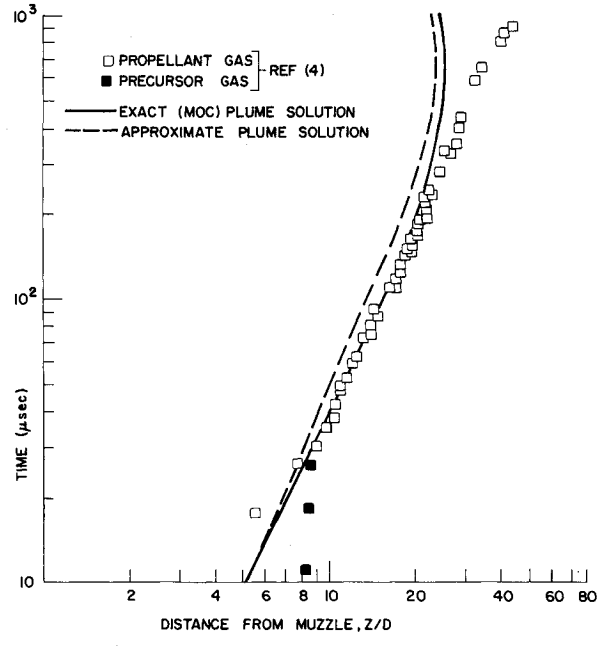

Fig. 7 Contact surface trajectory for M16.

The energy equation, in the form given by Eqs. (14) and (15), is solved by the second-order characteristic method previously described in connection with Eq. (12). (This technique was selected to minimize numerical diffusion of the entropy layers.)

The shock layer solution is completed by statement of initial conditions at $t=0$ or some other appropriate instant. In view of the type of experimental information available, the initial positions and velocities of the two shock waves and the contact surface are taken as the basic initial data. The initial flow conditions downstream of each shock are calculated from the shock jump conditions and the initial shock velocity. The initial pressure is assumed to vary linearly between the two shocks, and the initial velocity is assumed to vary linearly between each shock and the contact surface. In view of an anticipated behavior of the entropy layers, the logarithm of the entropy is assumed to vary linearly between each shock and the contact. The assumed values of the entropy on each side of the contact, which are invariant in time, were previously

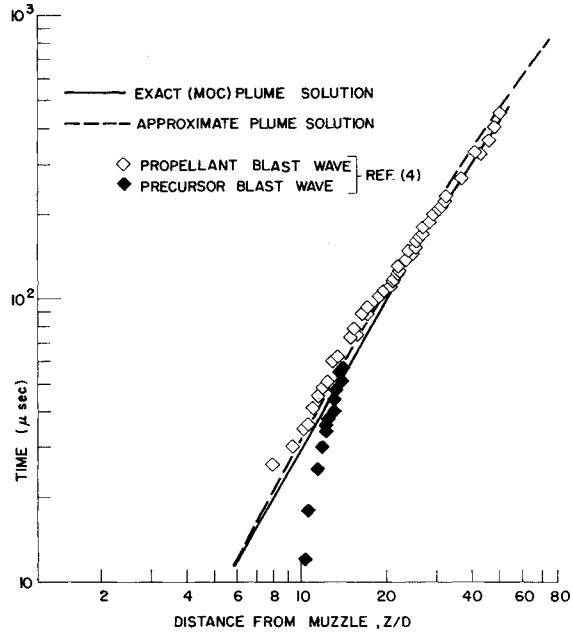

Fig. 8 Blast wave trajectory for M16.

discussed. As should be expected, the assumed form of the initial conditions affects the solution within a limited zone of influence, but the solution eventually becomes independent of the initial data and only dependent on the boundary conditions.

A comparison of the numerical solution obtained from the above shock layer analysis and the M16 data relative to the trajectories of the Mach disk, contact surface and blast wave is presented in Figs. 6-8, respectively. (It is pointed out that the described results were obtained using calclulated flow conditions at the muzzle of an M16 rifle provided by BRL. The calculated pressure variation compares favorably with experimental measurements.[3]) The position and velocity of the blast wave at $t=10$ μsec was estimated by extrapolating the data to this time in accord with the $n=3/5$ power-law indicated by blast theory. The contact surface data appears to follow an $n=1/2$ power-law which was used to extrapolate its initial position and velocity at $t=10$ μsec. Due to the interaction with the projectile, similar extrapolations of the Mach disk position and velocity are not possible. The Mach disk was assumed to be one diameter upstream of the contact at $t=10$ μsec and to have 10% smaller velocity. It is shown in Ref. 1 that perturbations as large as 20% in these estimated initial conditions bear negligible influence on the Mach disk trajectory after about 100 μsec, on the contact surface after 250 μsec, and on the blast wave after about 300 μsec.

Comparison of the Mach disk solution and experimental data in Fig. 6 clearly indicates that residual effects of the interaction with the projectile are very small after the projectile clears the Mach disk. At times earlier than 60 μsec, the data represent the base shock of the projectile rather than a Mach disk. It can be seen that in the time span $60<t<400$ μsec, the agreement between the data and the present theory, based on use of the exact (method of characteristics) plume solution, is excellent. However, the results utilizing the approximate plume Mach number distribution underestimate the Mach disk location by about 10-20% in the same time span. In the later time span $400<t<2000$ μsec, the present theory tends to overestimate the Mach disk location by about 20-30% (at worst). In view of the established inaccuracy of the approximate plume centerline Mach number distribution in the considered range of Mach disk positions, the agreement in this case between theory and data in the time span $400<t<2000$ μsec must be regarded as fortuitous. Although an error of 20-30% is not considered quantitatively serious in view of the approximations implicit in the present model, an explanation for the discrepancy in this time span will be discussed later.

Results are also presented in Fig. 6 for a calculation in which the origin of the spherical coordinate system was fixed at a position $z_o=0.2D$, corresponding to the effective origin of the blast field in Ref. 2. The agreement with experiment is somewhat less satisfactory in this case. However, no attempt has been made to systematically study the effect of varying the position of the moving origin from the presently proposed form, viz., $z_o=3/4z_f$.

As shown in Fig. 7, the trajectory of the contact surface (i.e., the inviscid interface between the propellant gases and the air) is accurately described by the present model for times less than about 200 μsec. An appreciable error is again attributable to use of the approximate plume solution. However, the theory predicts a slowdown in the rate of expansion of this front between 200 and 500 μsec and a small contraction between 500 and 1000 μsec, while the data shows a continual expansion of the front during the entire period of observation. Examination of the shadowgraph data (Fig. 1) indicates that the outer portions of the front tend to roll up into a vortex ring, which appears as a turbulent smoke ring. The data actually represent the trajectory of the front of this smoke ring, which may obscure the position of the contact surface at the axis but is evidently coincident with it at early time, e.g., $t<200$ μsec. The apparent continued forward motion of the front at $t>200$ μsec is believed to really be a broadening of the smoke ring surrounding the contact surface at the axis. It is emphasized that the contact surface in the present model is an inviscid surface of discontinuity whereas turbulent mixing along this interface is amply evident in the shadowgraphs. Relative to this point, it should be recognized that a substantial temperature discontinuity is generated along the contact surface which persists virtually unchanged after 200 μsec, but in reality is dissipated by turbulent mixing. Oxidation of unburnt propellant gases will also accompany the mixing of gases at this interface contributing to the characteristic "muzzle flash."

Referring to Fig. 8, it is indicated that the blast wave position at any instant during the period $30<t<100$ μsec is overestimated by about 10%, by the solution using the exact plume centerline information, although much better agreement is achieved after $t=150$ μsec. Since the blast wave is driven by the expanding spherical front represented by the contact surface, the outward displacement of the blast wave can be attributed to the outward displacement of the contact surface, which in turn can be related to the shift in the Mach disk location, associated with use of the exact plume centerline Mach number distribution. The sensitivity of the entire unsteady shock layer solution to the supersonic plume solution is therefore clearly demonstrated. The accuracy with which the Mach disk and contact surface trajectories are predicted for $t\leq400$ μsec can therefore be regarded as corroboration of the valicity of the quasi-steady supersonic plume model and the associated exact (method of characteristics) solution[10] thereof. The inaccuracy of the blast wave prediction for $t\leq150$ μsec is probably attributable to the evident flattening of the actual blast wave as compared to the assumed spherical shape of the theoretical blast wave during the time span in question. The actual blast wave gradually attains spherical symmetry further from the muzzle, bringing the theory and experiment into close agreement at later times, i.e., $t>150$ μsec. Note that the correlation of this data with spherical blast theory shown in Fig. 5 only pertains to the power-law exponent, $n=3/5$, as the constant B was selected to fit the data. The present solution also reproduces an $n=3/5$ variation in the time span $30<t<150$ μsec.

The typical variation of flow properties along the axis of the shock layer is indicated in Figs. 9-11 which pertain to $t=84.3$ μsec, when the projectile is within the shock layer. The entropy variation between the contact surface and the blast wave shown in Fig. 9 exhibits the characteristic entropy layer

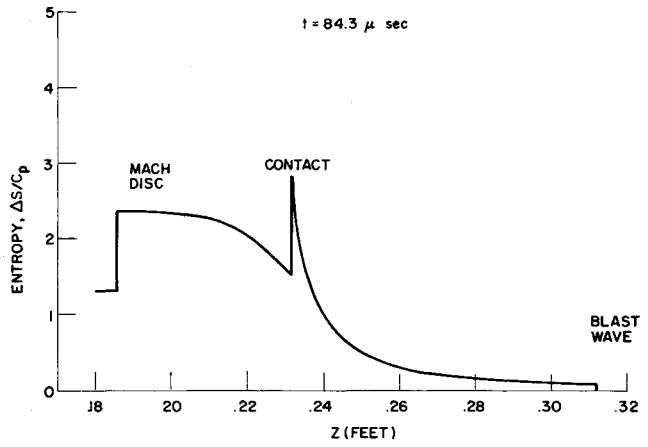

Fig. 9 Entropy variation between Mach disk and blast wave.

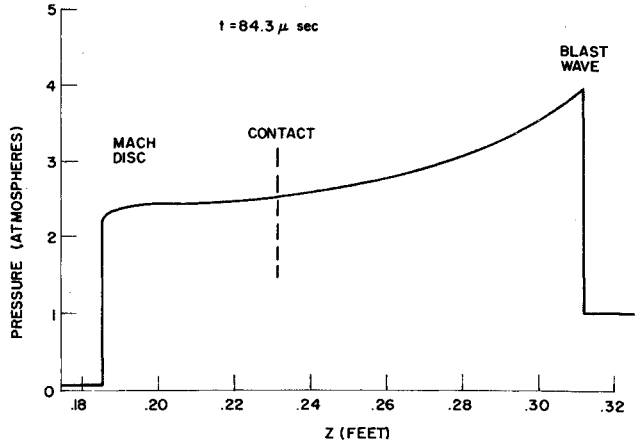

Fig. 10 Pressure field between Mach disk and blast wave.

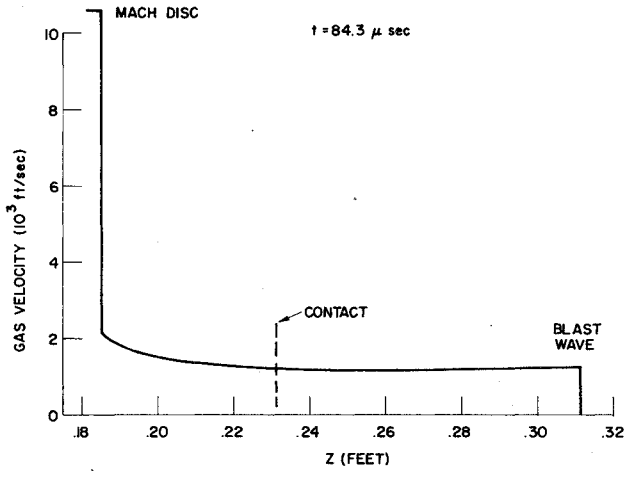

Fig. 11 Gas velocity distribution between Mach disk and blast wave.

behavior associated with blast wave theory and analogous steady, hypersonic flows. An interesting "inverse" entropy layer is formed between the Mach disk and contact, due to strengthening of the Mach disk with increasing distance from the muzzle. As shown in Figs. 10 and 11, the variations of pressure and velocity across the shock layer are relatively minor. Jumps in density and temperature occur at the contact corresponding to the entropy jump shown in Fig. 9.

The previously noted discrepancy between the predicted and observed Mach disk trajectory at later times, i.e., $t<400$ μsec, can now be tentatively attributed to one or both of the following possible causes. a) Erroneous information due to the over-displacement of the blast wave at early times could be slowly transmitted back to Mach disk through the subsonic shock layer and result in the noted error in the Mach disk location at later times. b) As the subsonic shock layer decays to atmospheric pressure and negligible gas velocity, the distance between the blast wave and the Mach disk continuously increases with a corresponding increase in the spacing of the finite difference grid and decrease in numerical accuracy, possibly resulting in a progressively increasing error. The latter possibility carries the more serious implication vis-a-vis prediction of the far field acoustic signature. As suggested in Ref. 1, it is probably appropriate to replace the present numerical solution at very late times (e.g., $t>2000$ μsec in the present example) by an asymptotic model incorporating a weak shock solution for the blast wave and a semi-empirical formula for the quasi-steady Mach disk (as confirmed for late times in Ref. 4). The possibility of accumulation of appreciable numerical error prior to the time when the previous approximations may be invoked can be avoided by periodic subdivision of the finite difference grid when a prescribed maximum grid size is met. This modification of the present computer program, and formulation of a consistent procedure for switching from the numerical shock layer solution for the near field to an analytical far field solution, to provide a uniformly valid model for the muzzle blast field, is planned.

Finally, it is noted that all the numerical results presented herein were obtained with a total of 14 grid points spanning the shock layer; each sub-layer contained 5 interior points and 2 boundary points. Several trial calculations were carried out with double the number of interior points, but the results were not significantly altered. Execution time on a CDC 6600 was under 13 sec to cover the time span from 10-2000 μsec for an M16 rifle, for which the cost was under $5.00, including input/output charges, at standard commercial rates.

Conclusions

A qualitative description of the gas-dynamics of muzzle blast has been presented in terms of well-known concepts from blast wave theory with variable energy release and highly underexpanded, steady jet plume analyses. The principal restrictions relative to the applicability of blast wave theory are the requirements of a power-law rate of energy deposition and of a spherically symmetric flowfield. In addition, the blast wave degenerates to a weak shock on the time scale of present interest and the blast theory representation must be modified accordingly. The effects of the rapidly varying pressure field generated by the blast wave on the supersonic plume exhausting from the muzzle are shown to be isolated from the flow between the barrel shocks up to the Mach disk. Representation of the plume is therefore simplified, and a quasi-steady model employing the axis Mach number variation from an exact (method of characteristics) solution is used herein. Comparisons with approximate plume solutions are also presented.

A numerical solution of the unsteady shock layer bounded by the Mach disk and blast wave is developed. Comparison of the numerical results with experimental measurements of the trajectories of the principal structural components of the blast field, viz., the Mach disk, contact surface and blast wave, generated by an M16 rifle shows generally excellent agreement and is considered satisfactory verification of the postulated model. A strong dependence of the shock layer on the accuracy of the plume solution is indicated. Matching of the present numerical solution for the near-field to an asymptotic far-field representation, vis-a-vis the acoustic signature, is suggested. It is pointed out that although a high degree of turbulent motion is evident in the shadowgraph data, the basic structural features of the blast flowfield appear well described by the present inviscid considerations, with the exception of an evident broadening of the interface between the propellant gases and the air at late times due to turbulent mixing.

References

[1] Erdos, J., Del Guidice, P., and Visich, M., "Aerodynamics of Sabot Discard Within a Muzzle Blast Environment," BRL CR149, April 1974, Ballistics Research Labs., Aberdeen Proving Ground, Md.

[2] Oswatitsch, K., "Intermediate Ballistics," Deutscheluft und Raumfahrt FB64-27, DVL Rept. 358, Dec. 1964, AD473-249.

[3] Schmidt, E. and Shear, D., "Flow Field About the Muzzle of an M16 Rifle," BRL Rept. 1692, Jan. 1974, Ballistic Research Labs., Aberdeen Proving Ground, Md.

[4] Schmidt, E. and Shear, D., *AIAA Journal*, Vol. 13, Aug. 1975, pp. 1088-1093.

[5] Sakurai, A., "Basic Development in Fluid Dynamics," edited by M. Holt, Academic Press, New York, 1965, pp. 309-375.

[6] Freeman, R. A., "Variable Energy Blast Waves," *Journal of Physics, Ph.D—Applied Physics*, Ser. 2, Vol. 1, 1968, pp. 1697-1710.

[7] Dabora, E. K., "Variable Energy Blast Waves," *AIAA Journal*, Vol. 10, Oct. 1972, pp. 1384-1385.

[8] Albini, F., "Approximate Calculation of Underexpanded Jet Structure," *AIAA Journal*, Vol. 3, Aug. 1965, pp. 1535-1537.

[9] Hubbard, E. W., "Approximate Calculation of Highly Underexpanded Jets," *AIAA Journal*, Vol. 4, Oct. 1966, pp. 1877-1878.

[10] Gerber, H., Private communication, Jan. 1974, Ballistic Research Labs., Aberdeen Proving Ground, Md.

[11] MacCormack, R., "The Effect of Viscosity in Hypersonic Impact Cratering," AIAA Paper 69-354, Cincinnati, Ohio, 1969.